Spin-polarized current separator based on a fork-shaped Rashba nanostructure

Xianbo Xiao[1,2] and Yuguang Chen[3†]

[1] School of Computer, Jiangxi University of Traditional Chinese Medicine, Nanchang 330004, China.
[2] Institute for Advanced Study, Nanchang University, Nanchang 330031, China.
[3] Department of Physics, Tongji University, Shanghai 200092, China.

E-mail: ygchen@tongji.edu.cn

Abstract.
    A scheme for a spin-polarized current separator is proposed by studying the spin-dependent electron transport of a fork-shaped nanostructure with Rashba spin-orbit coupling (SOC), connected to three leads with the same width. It is found that two spin-polarized currents are of the same magnitude but opposite polarizations can be generated simultaneously in the two output leads when the spin-unpolarized electrons injected from the input lead. The underlying physics is revealed to originate from the different spin-dependent conductance caused by the effects of Rashba SOC and the geometrical structure of the system. Further study shows that the spin-polarized current with strong a robustness against disorder, demonstrates the feasibility of the proposed nanostructure for a real application.

† Author to whom any correspondence should be addressed.

1. INTRODUCTION

In the past decades, spin-dependent electron transport in semiconductor nanostructures has drawn unprecedented attention because of its potential applications to semiconductor spintronics,[1] in which the electron spin rather than its charge is utilized for information processing. One of the primary tasks in the development of semiconductor spintronics is to be capable of generating and manipulating excess spin in semiconductor nanostructures, particularly by all electrical means. The Rashba spin-orbit coupling (SOC),[2] existing in asymmetric heterostructures and can be controlled by an external gate voltage,[3,4] may be an efficient method to satisfy this goal.

Various spin filtering devices have been proposed based on the Rashba semiconductor nanostructures without need for a magnetic element or an external magnetic field, such as T-shape electron waveguide,[5−9] quantum wires,[10−14] wire network,[15] two-dimensional electron gas (2DEG),[16] and quantum rings.[17−18] Recently, an interesting Fano-Rashba effect has been found in a straight quantum wire with local Rashba SOC.[19] This effect is attributed to the interference between the bound states formed by the Rashba SOC and the electrons in the conduction channel, giving rise to pronounced dips in the linear charge conductance. Apart from the SOC-induced bound states, the effects of structure-induced bound states on the electron and spin transport have also been concerned intensively.[6,20,21] In our recent works, we have investigated the spin-polarized electron transport properties of several typical Rashba quantum wires and found that they are very sensitive to the systems' longitudinal symmetry. Spin-polarized current can be generated in the longitudinally asymmetry systems when spin-unpolarized injections. Especially, the magnitudes of the spin polarization around the structure-induced Fano resonances are very large.[22,23] However, in the longitudinally symmetrical system no spin-polarized current can be achieved, despite the existence of the SOC- or/and structure-induced bound states.[24]

Inspired by the three works above, in this paper, we study the spin-dependent electron transport for a fork-shaped Rashba nanostructure with longitudinal-inversion symmetry. It is shown that two spin-polarized currents, with the same magnitude but different polarized directions, can be achieved in the two output leads in spite of spin-unpolarized injections and they still survive even in the presence of strong disorder. Therefore, a spin-polarized current separator device can be devised by using this system. The rest of this paper is organized as follows. In Section II, the theoretical model and analysis are presented. In Section III, the numerical results are illustrated and discussed. A conclusion is given in Section IV.

2. MODEL AND ANALYSIS

The investigated system in present work is schematically depicted in Fig. 1, where a 2DEG in the (x, y) plane is restricted to a fork-shaped nanostructure by a confining potential $V(x, y)$. The 2DEG is confined in an asymmetric quantum well, where the

Rashba SOC is assumed to play a dominantly role. The nanostructure consists of three narrow regions and a wide region. The wide region has a length L_2 and a uniform width W_2, while the narrow region has a length L_1 and a uniform width W_1, connected to a semi-infinite lead with the same width. The three connecting leads are normal-conductor electrodes without SOC, since we are only interested in spin-unpolarized injection. Such kind of Rashba system can be described by the spin-resolved discrete lattice model. The tight-binding Hamiltonian including the Rashba SOC on a square lattice is given as follow,

$$H = H_0 + H_{so} + V, \tag{1}$$

where

$$H_0 = \sum_{lm\sigma} \varepsilon_{lm\sigma} c^\dagger_{lm\sigma} c_{lm\sigma} - t \sum_{lm\sigma} \{ c^\dagger_{l+1m\sigma} c_{lm\sigma}$$
$$+ c^\dagger_{lm+1\sigma} c_{lm\sigma} + H.c \}, \tag{2}$$

$$H_{so} = t_{so} \sum_{lm\sigma\sigma'} \{ c^\dagger_{l+1m\sigma'} (i\sigma_y)_{\sigma\sigma'} c_{lm\sigma}$$
$$- c^\dagger_{lm+1\sigma'} (i\sigma_x)_{\sigma\sigma'} c_{lm\sigma} + H.c \}, \tag{3}$$

and

$$V = \sum_{lm\sigma} V_{lm} c^\dagger_{lm\sigma} c_{lm\sigma}, \tag{4}$$

in which $c^\dagger_{lm\sigma} (c_{lm\sigma})$ is the creation (annihilation) operator of electron at site (lm) with spin σ, $\sigma_{x(y)}$ is Pauli matrix, and $\varepsilon_{lm\sigma} = 4t$ is the on-site energy with the hopping energy $t = \hbar^2/2m^* a^2$, here m^* and a are the effective mass of electron and lattice constant, respectively. V_{lm} is the additional confining potential. The SOC strength is $t_{so} = \alpha/2a$ with the Rashba constant α. The Anderson disorder can be introduced by the fluctuation of the on-site energies, which distributes randomly within the range width w [$\varepsilon_{lm\sigma} = \varepsilon_{lm\sigma} + w_{lm}$ with $-w/2 < w_{lm} < w/2$].

In the ballistic transport, the spin-dependent conductance is obtained from the Landauer-Büttiker formula[25] with the help of the nonequilibrium Green function formalism.[26] In order to calculate the Green function of the whole system conveniently, the tight-binding Hamiltonian (1) is divided into two parts in the column cell

$$H = \sum_{l\sigma\sigma'} H_l^{\sigma\sigma'} + \sum_{l\sigma\sigma'} (H_{l,l+1}^{\sigma\sigma'} + H_{l+1,l}^{\sigma'\sigma}), \tag{5}$$

where $H_l^{\sigma\sigma'}$ is the Hamiltonian of the lth isolated column cell, $H_{l,l+1}^{\sigma\sigma'}$ and $H_{l+1,l}^{\sigma'\sigma}$ are intercell Hamiltonian between the lth column cell and the $(l+1)$th column cell with $H_{l,l+1}^{\sigma\sigma'} = (H_{l+1,l}^{\sigma'\sigma})^\dagger$. The Green function of the whole system can be computed by a set of recursive formulas,

$$\langle l+1|G_{l+1}|l+1 \rangle^{-1} = E - H_{l+1} - H_{l+1,l} \langle l|G_l|l \rangle H_{l,l+1},$$
$$\langle l+1|G_{l+1}|0 \rangle = \langle l+1|G_{l+1}|l+1 \rangle H_{l+1,l} \langle l|G_l|0 \rangle, \tag{6}$$

where $\langle l+1|G_{l+1}|l+1\rangle$ and $\langle l+1|G_{l+1}|0\rangle$ are respectively the diagonal and off-diagonal Green function, and

$$H_{l+1} = \begin{pmatrix} H_{l+1}^{\sigma\sigma} & H_{l+1}^{\sigma\sigma'} \\ H_{l+1}^{\sigma'\sigma} & H_{l+1}^{\sigma'\sigma'} \end{pmatrix}, \quad H_{l+1,l} = (H_{l,l+1})^\dagger = \begin{pmatrix} H_{l+1,l}^{\sigma\sigma} & H_{l+1,l}^{\sigma\sigma'} \\ H_{l+1,l}^{\sigma'\sigma} & H_{l+1,l}^{\sigma'\sigma'} \end{pmatrix}. \quad (7)$$

Utilizing the Green function of the whole system obtained above, the spin-dependent conductance from arbitrary lead p to lead q is given by

$$G_{pq}^{\sigma\sigma'} = e^2/hTr[\Gamma_p^\sigma G^r \Gamma_q^{\sigma'} G^a], \quad (8)$$

where $\Gamma_{p(q)} = i[\sum_{p(q)}^r - \sum_{p(q)}^a]$ with the self-energy from the lead $\sum_{p(q)}^r = (\sum_{p(q)}^a)^*$, the trace is over the spatial and spin degrees of freedom. $G^r(G^a)$ is the retarded (advanced) Green function of the whole system, which can be computed by the spin-resolved recursive Green function method,[23] and $G^a = (G^r)^\dagger$.

In the following calculation, the structural parameters of the system are fixed at $L_1 = L_2 = 10\ a$, $W_1 = 10\ a$, and $W_2 = 40\ a$. All the energy is normalized by the hoping energy $t(t = 1)$. And the z axis is chosen as the spin-quantized axis so that $|\uparrow> = (1,0)^T$ represents the spin-up state and $|\downarrow> = (0,1)^T$ denotes the spin-down state, where T means transposition. For simplicity, the hard-wall confining potential approximation is adopted to determine the boundary of the nanostructure since different confining potentials only alter the positions of the subbands and the energy gaps between them. The charge conductance and the spin conductance of z-component are defined as $G_{pq}^e = G_{pq}^{\uparrow\uparrow} + G_{pq}^{\uparrow\downarrow} + G_{pq}^{\downarrow\downarrow} + G_{pq}^{\downarrow\uparrow}$ and $G_{pq}^{Sz} = \frac{e}{4\pi} \frac{G_{pq}^{\uparrow\uparrow} + G_{pq}^{\downarrow\uparrow} - G_{pq}^{\downarrow\downarrow} - G_{pq}^{\uparrow\downarrow}}{e^2/h}$, respectively. Here the charge conductance means the transfer probability of electrons, and the spin conductance represents the change in local spin density between the input lead and the output lead caused by the transport of spin-polarized electrons.[27]

3. RESULTS AND DISCUSSION

In our numerical example, we choose the same material as that in Ref. [23], where the requirements of the parameters have been discussed. Figure 2 shows the electron energy (E) dependence of the charge and spin conductance when the spin-unpolarized electron injected from lead 1. The Rashba SOC strength $t_{so} = 0.19$. The step-like structures, oscillation caused by interference, and SOC-induced Fano resonance dips (see the red circles in Fig. 2(a)) can be found in the charge conductance. In addition, due to the system is longitudinally symmetrical, electrons have the same chance be transmitted to the different output leads. Therefore, as shown in Fig. 2(a) and (b), the charge conductance from lead 1 to 2 is the same as that from lead 1 to 3. However, the corresponding spin conductance from lead 1 to 2 is quite different from that from lead 1 to 3, as depicted in Fig. 2(c), the magnitudes of the spin conductance from the injecting lead to the two outgoing leads are always equal but their signs are contrary. In particular, a very large spin-polarized current can be generated at the structure-induced Fano resonances (such as $E = 0.16$, 0.44, etc.). It has demonstrated in our previous papers[22,23] that the magnitude of this spin-polarized current can be tuned by both the

strength of Rashba SOC and the structural parameters of the system so that we do not presented these results here.

The remarkable difference in the spin conductance between the upper and lower output leads can be utilized to design a spin-polarized current separator, i.e., if a spin-polarized current generated in one output lead, there must be another one in possession of the same magnitude but adverse polarized directions achieved in the other output lead. The physical mechanism of this device owing to the effect of the Rashba SOC and the geometrical structure of the system. The spin-dependent conductance from the input lead 1 to the output leads 2 and 3 as function of the electron energy is illustrated in Fig. 3(a) and (b), respectively. The strength of Rashba SOC is the same as that in Fig. 2. The fork-shaped Rashba nanostructure can be equivalently viewed as two coupled zigzag wire, whose longitudinal and transversal symmetries are broken.[12] So the relations $G_{12(3)}^{\uparrow\uparrow} = G_{12(3)}^{\downarrow\downarrow}$ and $G_{12(3)}^{\uparrow\downarrow} = G_{12(3)}^{\downarrow\uparrow}$ cannot be guaranteed, as shown in Fig. 3, leading to the nonzero spin conductance (see Fig. 2(c)) in respective lead. Furthermore, because the two output leads 2 and 3 lie symmetrically in the opposite direction with respect to the input lead 1, the total current must still be spin-unpolarized.[12,24] Therefore, the transmission probability of the spin-up (-down) electron from lead 1 to 2 always equals that of the spin-down (-up) electron from lead 1 to 3, that is, $G_{12}^{\sigma\sigma} = G_{13}^{\sigma'\sigma'}$ and $G_{12}^{\sigma\sigma'} = G_{13}^{\sigma'\sigma}$. As a consequence, the signs of the spin conductance from the lead 1 to leads 2 and 3 are contrary all along.

The above proposed spin-polarized current separator is based upon a perfectly clean system, where no elastic or inelastic scattering happens. However, in a realistic system, there are many impurities in the sample. The impurities in any semiconductor heterostructure may induce a random Rashba field, which gives rise to many new effects such as the realization of the minimal possible strength of SOC[28] and the localization of the edge electrons for sufficiently strong electron-electron interactions.[29] Thus the effect of disorder should be considered in practical application. The spin conductance from the input lead to the different output leads as function of the electron energy for (weak and strong) different disorders w are plotted in Fig. 4. The SOC strength is also set as $t_{so} = 0.19$. The spin conductance is destroyed when the impurities exist in the system and its magnitude become smaller with the increase of disorder. However, as shown in Fig. 4(c), the magnitude of the spin conductance around the structure-induced Fano resonances is still large when the disorder strength $w = 0.6$, which means that a comparatively large spin-polarized current can be obtained in the output leads even in the presence of strong disorder.

4. CONCLUSION

In conclusion, a scheme of a spin-polarized current separator is proposed by investigating the spin-dependent electron transport of a fork-shaped nanostructure under the modulation of the Rashba SOC. Two spin-polarized currents with the same magnitude but different polarizations can be generated synchronously in the two output leads

due to the distinct spin-dependent conductance results from the effects of SOC and the geometrical structure. The opposite spin-polarized currents can be generated and controlled by electrical means and they are robust against disorder. Thus the proposed nanostructure does not require the application of magnetic fields, external radiation or ferromagnetic leads, and has great potential for real applications.

References

[1]D. D. Awschalom, D. Loss, and Samarth N. *Semiconductor Spintronics and Quantum Computation*, (Springer, Berlin) 2002; I. Zutic, J. Fabian, and S. D. Sarma, Rev. Mod. Phys. **76** 323 (2004); J. Fabian, A. Matos-Abiague, C. Ertler, P. Stano, and I. Zutic, Acta Phys. Slov. **57** 565 (2007), and references therein.

[2]Y. A. Bychkov and E. I. Rashba, J. Phys. C **17** 6039 (1984).

[3]D. Grundler, Phys. Rev. Lett. **84** 6074 (2000).

[4]T. Koga, J. Nitta, T. Akazaki, and H. Takayanagi, Phys. Rev. Lett. **89** 046801 (2002).

[5]M. Yamamoto, T. Ohtsuki, and B. Kramer,Phys. Rev. B **72** 115321 (2005).

[6]F. Zhai and H. Q. Xu, Phys. Rev. B **76** 035306 (2007).

[7]S. Bellucci and P. Onorato, Phys. Rev. B **77** 075303 (2008).

[8]M. Yamamoto and B. Kramer, J. Appl. Phys., **103** 123703 (2008).

[9]T. Yokoyama and M. Eto, Phys. Rev. B **80** 125311 (2009).

[10]J.Ohe, M. Yamamoto, T. Ohtsuki, and J. Nitta, Phys. Rev. B **72** 041308(R) (2005).

[11]Q. F. Sun and X. C. Xie, Phys. Rev. B **71** 155321 (2005).

[12]Z. Y. Zhang, J. Phys: Condens. Matter **19** 016209 (2007).

[13] G. H. Liu and G. H. Zhou, J. Appl. Phys. **101** 063704 (2007).

[14] G. I. Japaridze, H. Johannesson, and A. Ferraz, Phys. Rev. B **80** 041308(R) (2009).

[15] H. X.Wang, S. J. Xiong, and S. N. Evangelou, Phys. Lett. A **356** 376 (2006).

[16] A. Pályi, C. Péterfalvi, and J. Cserti, Phys. Rev. B **74** 073305 (2006).

[17] P. Földi, O. Kálmán, M. G. Benedict, and F. M. Peeters, Phys. Rev. B **73** 155325 (2006).

[18] P. Földi, O. Kálmán, M. G. Benedict, and F. M. Peeters, Nano Lett. **8** 2556 (2008).

[19] D. Sánchez and L. Serra, Phys. Rev. B **74** 153313 (2006).

[20] Y. P. Chen, X. H. Yan, and Y. E Xie, Phys. Rev. B **71** 245335 (2005).

[21] Y. P. Chen, Y. E Xie, and X. H. Yan, Phys. Rev. B **74** 035310 (2006).

[22] X. B. Xiao, X. M. Li, and Y. G. Chen, Phys. Lett. A **373** 4489 (2009).

[23] X. B. Xiao and Y. G. Chen, Europhys. Lett. **90** 47004 (2010).

[24] X. B. Xiao, X. M. Li, and Y. G. Chen, ACTA PHYSICA SINICA **58** 7909 (2009).

[25] M. Büttiker, Phys. Rev. Lett. **57** 1761 (1986).

[26] L. W. Molenkamp, G. Schmidt, and G. E.W. Bauer, Phys. Rev. B **62** 4790 (2000); T. P. Pareek and P. Bruno, Phys. Rev. B **63** 165424-1 (2001).

[27] D. V. Khomitsky, Phys. Rev. B **79** 205401 (2009).

[28] E. Ya. Sherman, Phys. Rev. B **67** 161303(R) (2003).

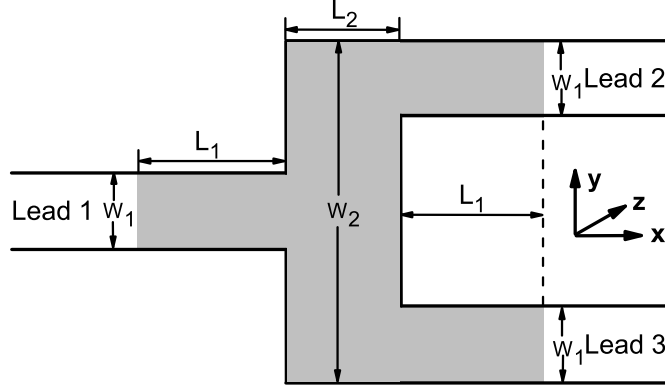[29] A. Ström, H. Johannesson and G. I. Japaridze, Phys. Rev. Lett. **104** 256804 (2010).

Figure 1. Schematic diagram of the fork-shaped nanostructure with Rashba SOC. The narrow regions have the same length L_1 and width W_1, while the wide region has another length L_2 and width W_2.
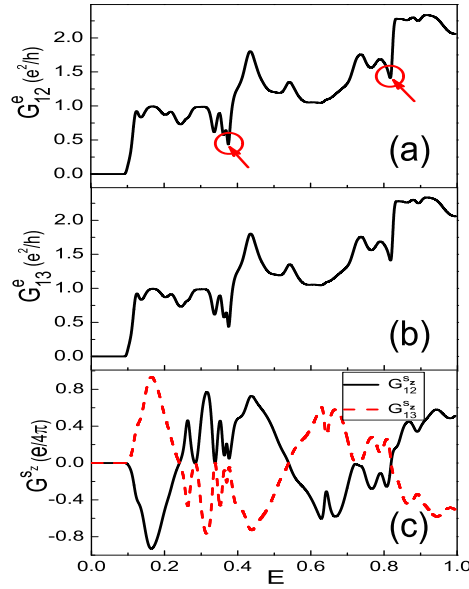

Figure 2. (Color online) Conductance spectra of a fork-shaped Rashba nanostructure as function of the electron energy for spin-unpolarized electron injections: (a) the charge conductance from lead 1 to 2; (b) the charge conductance from lead 1 to 3; (c) the corresponding spin conductance from lead 1 to 2 (the solid line) and 3 (the dash line). The Rashba SOC strength $t_{so} = 0.19$.
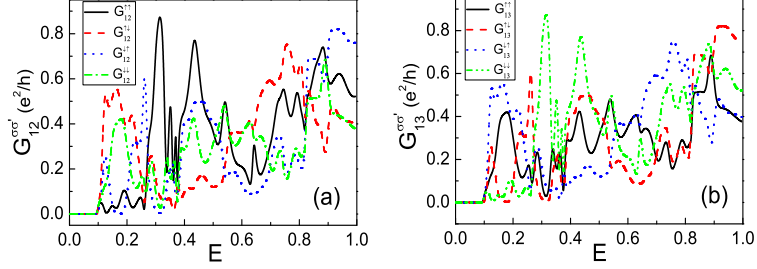
Figure 3. (Color online) The calculated spin-dependent conductance as function of the electron energy when the spin-unpolarized electron travels from lead 1 to 2 (a) and 3 (b). The Rashba SOC strength is the same as that in Fig. 2.
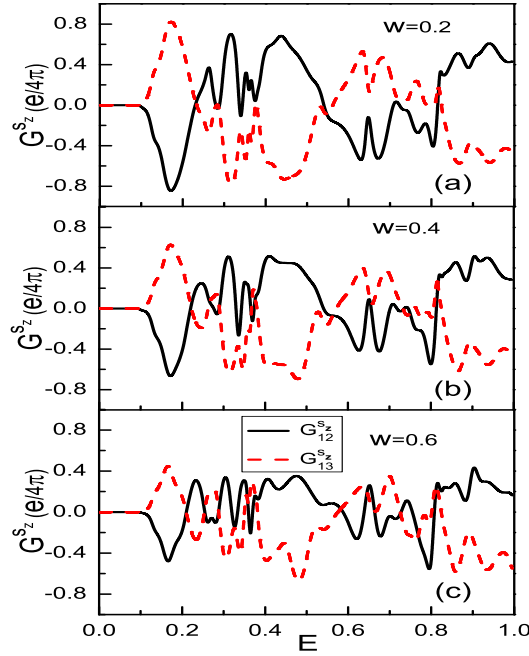

Figure 4. (Color online) The calculated spin conductance as function of the electron energy for different disorder strengths. The solid line represents G_{12}^{Sz} and the dashed line G_{13}^{Sz}. The Rashba SOC strength is the same as that in Fig. 2.